EVALUATING THE FATIGUE LIFE OF STEEL BRIDGES USING FIELD MEASUREMENTS

JEREMIAH FASL

BIOGRAPHY

Dr. Jeremiah Fasl is an Associate III at Wiss, Janney, Elstner Associates, Inc.

Dr. Todd Helwig is an Associate Professor at The University of Texas at Austin.

Dr. Sharon Wood is the Interim Dean of the Cockrell School of Engineering and Professor in Engineering at The University of Texas at Austin.

Mr. Richard Lindenberg is a Senior Associate at Wiss, Janney, Elstner Associates, Inc.

SUMMARY

Highway bridges provide vital links in the transportation network, supplying routes for daily commutes and the infrastructure needed to supply goods and services. Under the pressure of reduced budgets and an aging infrastructure, transportation officials face the difficult task of maintaining the nation's inventory of highway bridges. In terms of steel bridges, one of the critical types of structural deterioration is fatigue-induced fracture.

Methodologies that enable engineers to collect quantitative information on fatigue behavior of steel bridges by monitoring the service-load response will be presented. A simple method, index stress range, for normalizing fatigue data as a means to express fatigue accumulation in terms of a single parameter will be discussed. The method facilitates comparisons among multiple strain gages positioned along the same bridge and can also be used to compare the accumulation rate of fatigue damage among bridges within an inventory of bridges. Finally, deterministic and probabilistic methods for calculating the remaining fatigue life will be presented.

Evaluating the Fatigue Life of Steel Bridges Using Field Measurements

Introduction

Highway bridges provide vital links in the transportation network, supplying routes for daily commutes and the infrastructure needed to supply goods and services. Under the pressure of reduced budgets and an aging infrastructure, transportation officials face the difficult task of maintaining the nation's inventory of highway bridges. In terms of steel bridges, one of the critical types of structural deterioration is fatigue-induced fracture.

If fracture is allowed to occur, localized damage can propagate to member failure or even bridge collapse. As more bridges near or exceed their intended design lives, transportation officials must make decisions on which bridges can be safely kept in service and which need to be replaced or retrofitted. The primary method used to identify structural deterioration is hands-on visual inspections. The inspections provide transportation officials with qualitative data related to the number of cracks and rate of crack growth, but quantitative data are often needed to distinguish among the bridges in an inventory.

Calculating the remaining fatigue life is one means of providing quantitative data to transportation officials. To estimate the remaining fatigue life of a bridge, the fatigue damage must be characterized using either the results of structural analysis or measured strains. Field monitoring provides a direct measure of the spectrum of stress ranges at the location of a strain gage, whereas values for the representative fatigue truck, live load distribution factors among girders, and dynamic impact factor must be assumed to calculate the stress range using structural analysis. As such, the use of measurements from strain gages eliminates some of the assumptions that need to be made and minimizes the uncertainty. By minimizing the uncertainty, a more representative remaining fatigue life can be estimated.

Methodologies that enable engineers to collect quantitative information on fatigue behavior of steel bridges by monitoring the service-load response will be presented. A simple method, index stress range, for normalizing fatigue data as a means to express fatigue accumulation in terms of a single parameter will be discussed. The method facilitates comparisons among multiple strain gages positioned along the same bridge and can also be used to compare the accumulation rate of fatigue damage among bridges within an inventory of bridges. Finally, deterministic and probabilistic methods for calculating the remaining fatigue life will be presented.

Background

Before 1970, the fatigue guidelines in the AASHTO bridge design specifications were based on the measured response of specimens that were generally tested under constant-amplitude loading (1). These tests revealed that the primary variables affecting fatigue life were the stress range and configuration of the connection detail (1). In addition, a stress range was identified, the constant-amplitude fatigue limit (CAFL), S_{th}, below which the fatigue life was expected to be infinite. These concepts serve as the basis for the S-N curves (Figure 1) used in the current bridge design specifications in the US (2).

According to the AASHTO Load and Resistance Factor Design (LRFD) Bridge Design Specifications (2), the number of cycles to failure, N_f, for a given constant-amplitude stress range, S_r,, is calculated using Eq. 1:

$$N_f = \frac{A}{S_r^3} \qquad \text{Eq. 1}$$

where A is the fatigue constant for the detail category defined by AASHTO (2). Because Eq. 1 is used for the design of new bridges, the fatigue constant for each detail category corresponds to a low probability of failure. As a
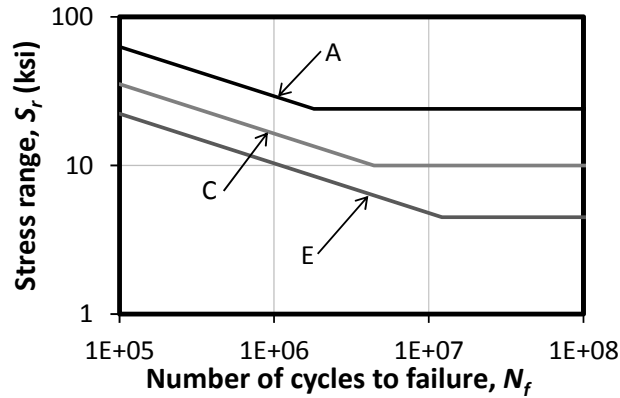
Figure 1*:* **Representative S-N design relationships from AASHTO (2).**

result, the median fatigue life of a population of nominally-identical connections is considerably greater than N_f.

Although fatigue tests have traditionally been conducted using a constant-amplitude stress range, highway bridges are subjected to stress cycles with varying amplitudes under service loads. A cumulative damage theory is used to relate the fatigue damage from variable-amplitude stress cycles to the fatigue damage from constant-amplitude stress cycles. The most common damage theory is Palmgren-Miner's rule (3), which is based on a linear damage hypothesis. The Palmgren-Miner rule for linear damage accumulation is simple to use, and the results agree with experimental data (3). Nonlinear cumulative damage theories have been proposed (i.e. (4)); however, the equations are more complicated to use, and the results are not consistently better than a linear damage model (3).

Using Palmgren-Miner's rule, the fatigue damage induced by a spectrum of stress cycles can be related to a single, equivalent stress range (1), which is represented by Eq. 2:

$$S_{re} = \left(\sum_{j=1}^{k} \frac{n_j}{n_m} S_{rj}^3 \right)^{1/3} \qquad \text{Eq. 2}$$

where S_{re} is the effective stress range, n_j is the number of stress cycles imposed with a stress range of S_{rj}, and n_m is the total number of stress cycles. For data collected using strain gages, the total number of stress cycles within the stress

spectrum can be calculated using the rainflow counting algorithm to evaluate the measured strain history.

The effective stress range is a useful metric because it can be used to calculate the remaining fatigue life, as discussed in (5). One of the limitations of this traditional approach for evaluating the accumulation of fatigue damage is that both the effective stress range and the total number of cycles experienced during the service life of the bridge must be used to characterize the fatigue damage at a given location. However, both of these parameters vary with location along the bridge, which complicates comparison of fatigue data from multiple sensors using the effective stress range as the sole parameter.

To illustrate that limitation, the effective stress range and number of cycles for three representative gage locations are presented (Figure 2). To compare gage locations, the proportion of the design life that has been consumed by the imposed loading cycles (D) can be used as a metric, which will plot parallel to the design fatigue life. Because both the effective stress range and number of cycles are larger for gage (b) than for gage (a), it is obvious that gage (b) has a higher accumulation of damage (D) than gage (a). Likewise, because the number of cycles for gage (c) is larger than gage (a) while the effective stress ranges are equal, gage (c) has a higher accumulation of damage than gage (a). Nonetheless, comparing the relative accumulation of damage between gages (b) and (c) is more complicated. Gage (b) has a higher effective stress range, but a fewer number of cycles, than gage (c). Using historical methods of evaluating fatigue, the only way to compare the two gage locations would be to calculate the remaining fatigue life or plot the damage accumulation ratio (Figure 2). A new approach, index stress range, which is discussed in the next section, was developed to quantify the relative accumulation of damage between gages.

Index Stress Range

The index stress range method was proposed by (6) as a means of expressing the fatigue damage accumulation in terms of a single parameter.
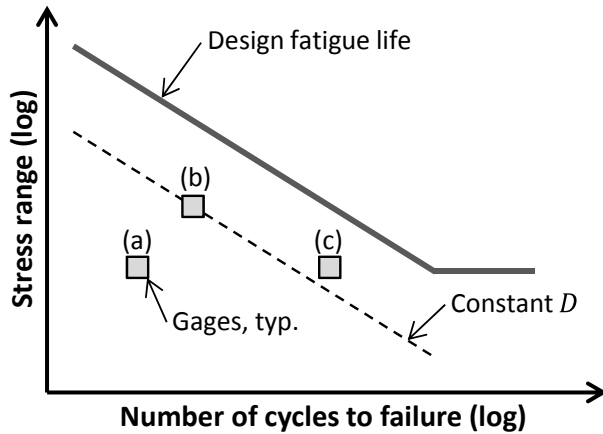
Figure 2: Comparison of relative damage levels for three gage locations.

This method facilitates comparisons among multiple strain gages positioned along the same bridge and can also be used to compare the accumulation rate of fatigue damage among bridges within an inventory of bridges. By normalizing the data to an index stress range, the number of cycles at the selected stress range becomes the direct metric of relative fatigue damage: twice as many cycles at the same index stress range causes twice the fatigue damage.

The full derivation of the method is provided in (5). As a first step, the engineer selects the value of the index stress range, $\hat{S}_{ri}$, to be used in the calculations. Although the choice is arbitrary, the constant-amplitude fatigue limit, S_{th}, is a convenient choice. Then the effective number of cycles at the index stress range, $\hat{n}_i$, is calculated such that the accumulated fatigue damage induced is the same as that induced by the measured stress spectrum:

$$\hat{n}_i(S_{ri}) = \sum_{j=1}^{k} n_j \frac{S_{rj}^3}{\hat{S}_{ri}^3} \qquad \text{Eq. 3}$$

The advantages of using the index stress range will be presented later using data from a fracture-critical bridge.

Remaining Fatigue Life

Metal fatigue is not a simple process; rather it involves localized damage as the metal is subjected to cyclic loading, which causes variability in the fatigue resistance. The fatigue life of a particular bridge depends on the inherent variability of the fatigue response of the connection details, the rate of accumulation of fatigue cycles (past, current, and future), and the method of calculation. The fatigue life of bridge components can be estimated using either deterministic or probabilistic approaches. Deterministic approaches do not directly include uncertainty in the analysis, yet using those approaches, the remaining fatigue life is easy to calculate and understand. In contrast, probabilistic approaches provide a method for including many types of uncertainty in the analysis, but the results are not as easily understood.

The current design fatigue relationship given by the AASHTO LRFD Specifications (2) is based on experimental tests of typical steel connections subjected to a constant-amplitude stress range (S-N curves). The design number of cycles to failure for a given stress range (S_r) was presented previously (Eq. 1), which corresponds to a design value. The mean number of cycles until failure ($\bar{N}_f$) can also be calculated if the mean value of the fatigue constant (μ_A) is used rather than the design value (Eq. 4).

$$\bar{N}_f = \frac{\mu_A}{S_r^3} \qquad \text{Eq. 4}$$

The design and mean values of the fatigue constant for each AASHTO fatigue category are summarized in Table 1. The two values can produce significantly different values for the number of cycles to failure. For instance, the design numbers of cycles to failure (N_f) at 5 ksi for a Category E detail is 8.8 million, whereas the mean number of cycles to failure ($\bar{N}_f$) is 13.6 million. Thus, the mean number of cycles to failure is more than 1.5 times the design value for a detail characterized as Category E.

Though the fatigue damage induced during a particular period of time can be obtained directly from field measurements, it is the accumulated damage over the service life of the bridge that influences the fatigue life. In general, traffic volume is irregular; it can increase or decrease in a given year, day, or hour due to weather, accidents, and many other sources, which makes modeling actual traffic patterns nearly

Table 1: Fatigue constant (A), mean fatigue constant (μ_A), and constant-amplitude fatigue limit (CAFL) for each fatigue detail category (2).

AASHTO Fatigue Category	Fatigue constant (ksi³)		CAFL (ksi)
	A (code value)	μ_A (mean value)	
A	250×10^8	719×10^8	24.0
B	120×10^8	237×10^8	16.0
B′	61×10^8	117×10^8	12.0
C	44×10^8	93×10^8	10.0
C′	44×10^8	93×10^8	12.0
D	22×10^8	44×10^8	7.0
E	11×10^8	17×10^8	4.5
E′	3.9×10^8	7.5×10^8	2.6

impossible. The goal then is to use a traffic model that on average is representative of the actual traffic patterns. A given traffic model can be validated if multiple years of traffic data (Average Annual Daily Traffic (AADT) from counting strips) or measured strain data are available. If the traffic model cannot be validated, a couple traffic models can be assumed, and the fatigue life can be bounded.

Geometrical traffic growth at an annual rate between 2% and 6% is typically considered to be more realistic than zero growth (constant traffic volume over the design life of the bridge), and is the range of growth rates recommended by the AASHTO Manual for Bridge Evaluation (7). Nonetheless, due to limitations on traffic volume, traffic growth will likely not increase indefinitely; therefore, some restraint should be exercised when considering long periods of time (greater than 30 years). The AASHTO LRFD Specifications (2) suggest an upper bound of 20,000 vehicles per lane per day to cap projected growth. As an alternative, historical data (counting strips) may provide a more realistic model to use.

Deterministic Approach

Using a deterministic approach to estimate fatigue life, the fatigue life (m) depends on the stress range (S_r); the current traffic volume (N_{yk}); the current age of the bridge (k); the assumed annual rate of increase in traffic volume (r); and the AASHTO detail category constant for the bridge (A), as seen in Eq. 5. The full derivation of Eq. 5 can be found in (5).

$$m = \frac{\log\left(\frac{r \times A}{N_{yk} \times S_r^3}(1+r)^{(k-1)} + 1\right)}{\log(1+r)} \quad \text{Eq. 5}$$

If Eq. 5 is used, the design value of the fatigue constant (A) corresponds to a 5th percentile value (approximately 95% of the connection details will sustain more cycles than the design value before failure). In contrast, the mean values correspond to a probability of failure of approximately 50%. The AASHTO Manual for Bridge Evaluation (7) recommends calculating the fatigue life at an "evaluation" life, which is one standard deviation below the mean and corresponds to a probability of failure of approximately 15%. The "evaluation" life can be calculated using a fatigue constant that is one standard deviation below the mean. Because the annual growth rate (r) and stress range (S_r) must be approximated by the engineer, the probabilities of failure are approximate. The stress range (S_r) and current traffic volume (N_{yk}) used in this analysis should correspond to the damage in year k. As such, either the index stress range (S_{ri}) and number of cycles at the index stress range ($N_{y,i}(S_{ri})$) in year k can be used, or the effective stress range (S_{re}) and corresponding number of measured cycles ($N_{y,m}$).

Probabilistic Approach

Due to the uncertainty in calculating the fatigue life, reliability equations may be a more appropriate calculation method. To solve for the

remaining fatigue life using a probabilistic approach, a fatigue limit state function must be considered. For this fatigue limit state, failure corresponds to fracture (rapid propagation of a crack) of a critical bridge detail. Following the derivation presented in (5) and (8), the reliability index (β) can be calculated using Eq. 6:

$$\beta = \frac{\lambda_\Delta + \lambda_A - 3 \times \ln(S_{ri}) - \lambda_{N_b(t)}}{\sqrt{\zeta_\Delta^2 + \zeta_A^2 + \zeta_{N_b(t)}^2}} \qquad \text{Eq. 6}$$

$$\lambda_{N_l} = \ln(\mu_{N_b(t)}) - \frac{\zeta_{N_b(t)}^2}{2} \qquad \text{Eq. 7}$$

$$\zeta_{N_b} = \sqrt{\ln\left(1 + \left(\frac{\mu_{N_b(t)}}{\sigma_{N_b(t)}}\right)^2\right)} \qquad \text{Eq. 8}$$

where λ_Δ and ζ_Δ are the lognormal parameters that account for the variability of using Palmgren-Miner's rule to relate variable-amplitude stress ranges to constant-amplitude fatigue data (8); where λ_A and ζ_A are the lognormal parameters that account for the variability of the fatigue constant (A); S_{ri} is the index stress range; and $\lambda_{N_b(t)}$ (Eq. 7) and $\zeta_{N_b(t)}$ (Eq. 8) are the lognormal parameters for the number of cycles at the index stress range. For this paper, $\lambda_\Delta = 0.0$ and $\zeta_\Delta = 0.163$ were assumed, which is consistent with (8). The lognormal parameters for the fatigue constant

are summarized in Table 2.

The number of cycles at the index stress range at a specific year t varies with the number of cycles in the first year of service ($\mu_{N_b(1)}$) and the assumed rate of growth (r), as seen in Eq. 9:

$$N_b = \mu_{N_b(1)} \frac{(1+r)^t - 1}{r} \qquad \text{Eq. 9}$$

The mean fatigue damage from the current year (k) of service, obtained from measurements, can be used to approximate the damage from the first year by using Eq. 10.

$$\mu_{N_l} = \frac{\mu_{N_b(k)}}{(1+r)^{k-1}} \qquad \text{Eq. 10}$$

Finally, the probability of failure for a given year can be calculated using Eq. 11.

$$P_F = \Phi(-\beta) \qquad \text{Eq. 11}$$

Description of Bridge

A three-span, twin plate-girder bridge was instrumented with strain gages to evaluate its fatigue performance. The bridge is along a major transportation corridor with significant truck traffic. The critical connections were added to the bridge when it was widened more than 35 years ago. The bridge is considered to be fracture critical because the superstructure

Table 2: Variation in fatigue constant (A) from (7) and derived parameters for lognormal distribution.

AASHTO Fatigue Category	Fatigue constant		σ_A	Parameters for lognormal distribution	
	A (code value)	μ_A (mean value)		λ_A	ζ_A
A	250×10^8	719×10^8	1.64	25.0	0.49
B	120×10^8	237×10^8	1.38	23.9	0.32
B′	61×10^8	117×10^8	1.35	23.2	0.30
C	44×10^8	93×10^8	1.42	23.0	0.35
C′	44×10^8	93×10^8	1.42	23.0	0.35
D	22×10^8	44×10^8	1.38	22.2	0.33
E	11×10^8	17×10^8	1.25	21.3	0.22
E′	3.9×10^8	7.5×10^8	1.35	20.4	0.30
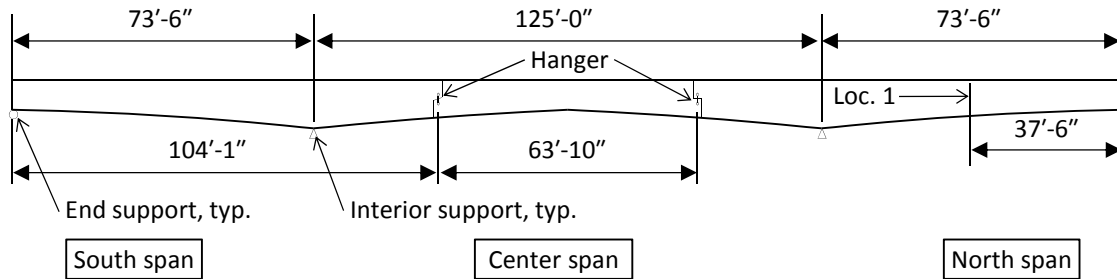
Figure 3*: **Elevation of the bridge and location of the strain gages. Strain gages were installed at Location 1 on both sides of the top flanges of the longitudinal girders.**

includes only two longitudinal girders and the failure of a flange from one girder would be expected to lead to the collapse of the entire bridge. The total length of the bridge is 272 ft, with 73.5-ft end spans and a 125-ft center span. The longitudinal girders in the end spans are continuous over the interior supports and extend 30.6 ft into the center span (Figure 3). Because the center section is suspended by hangers between the cantilevers in the middle span, the bridge is statically determinate.

Strain gages were installed at multiple locations along the length of the bridge on the top and bottom flanges. However, the focus of this paper is on data gathered from gages installed on the top flanges of the longitudinal girders at Location 1 (Figure 3). One of the gages was located on the east edge of the west girder, and one of the gages was located on the west edge of the east girder. Because data from only two gages are presented, the gages will be referred to by the specific girder on which the gage was installed, west girder or east girder. Location 1 corresponds to an AASHTO Category E detail. To measure the nominal response of the girder (matches assumption of AASHTO S-N curve), the gages were installed 2 ft away from the stiffener angles. The complete set of strain data is presented in (5).

Prior to the bridge being widened, traffic travelled in both the northbound and southbound directions; after the widening, traffic only travelled in the northbound direction. Over the entire life of the bridge, the majority of the trucks are expected to have crossed the bridge in the right lane, which is supported by the east girder.

At the location of the strain gages, negative moment is induced when a vehicle is in the center span, and positive moment is induced when a vehicle is in the north span. The difference in strain readings between the maximum positive and maximum negative readings determines the maximum stress range for a given vehicle crossing the bridge.

Measured Response of Bridge

The maximum-measured stress ranges from the strain gages were larger than the CAFL; therefore, this bridge is expected to have a finite fatigue life. The index stress range can be used to compare the two sets of stress spectra presented in Figure 4. Using an index stress range equal to S_{th} (4.5 ksi for Category E details (2)), the east girder experienced an average of 6,070 equivalent stress cycles per day, compared to an average of 1,250 equivalent stress cycles for the west girder. The advantage of the index stress range is that the engineer can immediately determine that 4.9 (6,070/1,250) as much fatigue damage accumulated in the east girder than the west girder during the monitoring period.

If a different value had been selected for the index stress range, the number of equivalent stress cycles would be different, but the fatigue damage accumulation ratio for each girder would remain unchanged. Therefore, direct comparisons of the relative amount of fatigue damage are always possible.
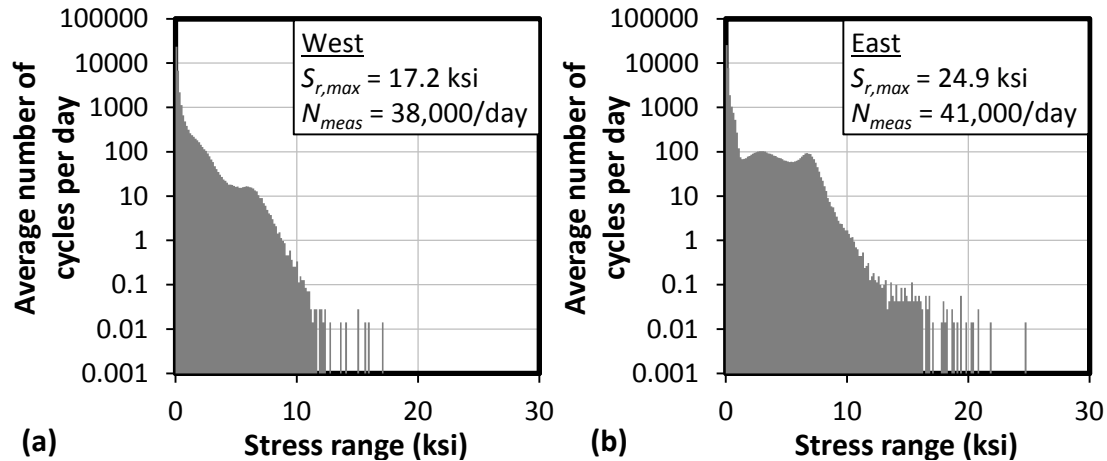
Figure 4: Stress spectra calculated from the strain histories recorded from the top flange of the (a) west girder and (b) east girder.

Remaining Fatigue Life (Deterministic)

The field-measured data were used to calculate the fatigue life using the deterministic method discussed previously. To evaluate the remaining fatigue life, the damage in year 1 was estimated using different annual growth rates. As seen in Table 3 there is considerable difference in the amount of damage calculated in the first year of service for assumed rates of traffic growth between 2% and 6%. For both gage locations, the extrapolated fatigue damage in the first year for an assumed annual growth rate of 2% is four times larger than the damage for an annual growth rate of 6%.

The fatigue lives were calculated for the west and east girders (Table 4). The age of the bridge connection was 37 years at the time of the calculation. As seen in Table 4 the design and mean fatigue lives have both been exceeded in the east girder, which corresponds to a negative fatigue life. The mean fatigue life in the east girder has been far exceeded if the 2% annual growth rate is correct. If the 6% growth rate is more representative of traffic growth, the mean fatigue life has still been exceeded, but not by as many years.

Based on the calculations, the west girder has a longer fatigue life than the east girder. The design fatigue life of the west girder has only been exceeded for 2% annual growth. For the other two growth rates, the fatigue life has not been exceeded for the design and mean calculation levels.

Remaining Fatigue Life (Probabilistic)

The probability of failure for a given year can be calculated using the probabilistic approach. The approach allows a bridge owner to evaluate the risk of keeping a bridge in service for a given duration and probability of failure. The fatigue life from the probability of failure can be compared to other methods by determining the year when a given level (i.e. 5%, 50%, etc.) is crossed. Unlike the deterministic methods, the probabilistic method considers uncertainty in the fatigue damage. The uncertainty in the fatigue damage in year 37 is summarized in Table 5.

The probabilistic approach was applied to the west and east girders (Figure 5). Comparing the two locations, the east girder has a higher probability of failure than the west girder for any given year. This is expected since more damage occurred in the east girder than the west girder during the monitoring period.

Because the annual rate of growth is not known for the bridge, a range of growth rates (2% to 6%) was considered. If the 2% model of annual growth is correct, the probability of failure for the current age of the bridge is nearly 100% for the east girder. If 6% growth is correct, the probability of failure is 95%.

Table 3: Fatigue damage in year 37 and extrapolated damage in year 1 for annual growth rates of 2%, 4%, and 6%.

Annual growth	West girder		East girder	
	$\bar{N}_{d,i}(4.5ksi)$ in year 1	$\bar{N}_{d,i}(4.5ksi)$ in year 37	$\bar{N}_{d,i}(4.5ksi)$ in year 1	$\bar{N}_{d,i}(4.5ksi)$ in year 37
2%	610	1,250	2,990	6,070
4%	300	1,250	1,480	6,070
6%	150	1,250	750	6,070

Table 4: Calculated fatigue life in years for the west and east girders using the deterministic approach.

P_F	West girder			East girder		
	2%	4%	6%	2%	4%	6%
5% (design)	37	43	45	10	16	22
50% (mean)	50	52	52	15	22	27

Table 5: Mean and standard deviation in year 37 for the west and east girders.

	$\mu_{\bar{N}_{d,i}(4.5ksi)}$ in year 37	$\sigma_{\bar{N}_{d,i}(4.5ksi)}$ in year 37
West girder	1,250	113
East girder	6,070	526
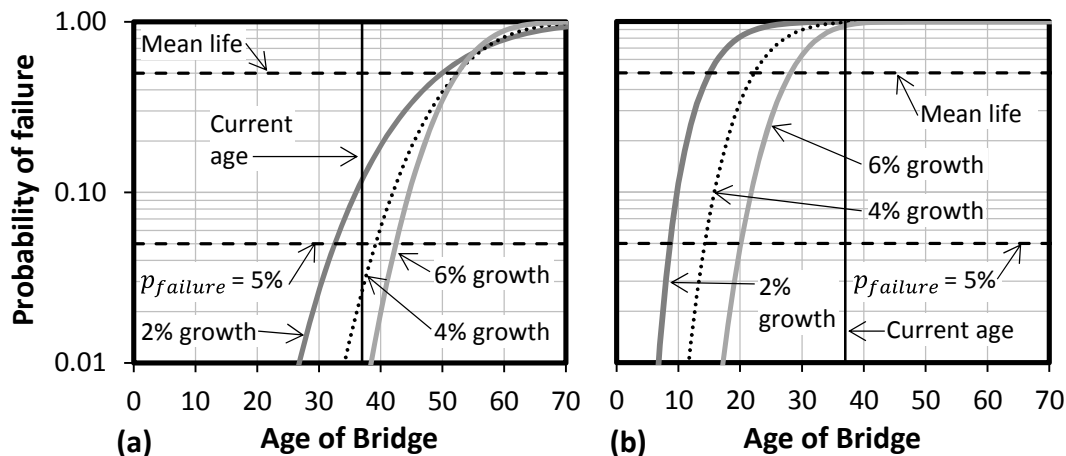
Figure 5: Probability of failure in the (a) west and (b) east girders.

For the west girder, the probability of failure is between 0.5% and 11% in year 37. As can be seen in Figure 5. 2% growth will have a higher probability of failure for years prior to the current age of the bridge and slightly into the future. Though, in year 55 and beyond that point, 6% growth has a greater probability of failure as the accumulated cycles for 6% growth exceed 2% growth.

Discussion and Conclusions

In terms of estimating the remaining fatigue life, there is much uncertainty. Traffic patterns can change drastically from hour to hour, day to day, and year to year. Weather, traffic accidents, and many other sources affect the accumulation of traffic and fatigue damage at a bridge. The deterministic and probabilistic approaches

produced comparative fatigue lives for the two probability levels (5% and 50%) for all growth rates. The fatigue lives in the east girder were closer between the deterministic and probabilistic approaches, because the uncertainty in the current level of fatigue damage did not have as large of an influence on the calculation of fatigue life. In contrast, the uncertainty had more of an influence on the fatigue life for the west girder, which is why the fatigue life for the probabilistic method had a lower fatigue life than the deterministic approach, in general. If the uncertainty from determining the fatigue damage is small, deterministic and probabilistic methods can provide comparable results. Though, using a deterministic approach, the calculated fatigue life corresponds to a limited number of probabilities of failure (5% and 50%).

The probabilistic method provides the framework for calculating the risk of keeping a bridge in service. Risk involves making decisions with the possibility of loss. With the probability of failure calculated for each year, the owner can weigh the potential cost from collapse or failure with the cost from replacing the bridge. The loss can take into account user costs from the bridge being closed, cost of bridge replacement, and cost of additional inspections. Knowing all of these costs, the owner can determine the optimal point of replacing the bridge and/or increasing the rate of inspections to minimize the loss to the public.

Acknowledgments

References

(1)   Schilling, C., Klippstein, K., Barsom, J., and Blake, G. (1978). *Fatigue of Welded Steel Bridge Members Under Variable-Amplitude Loadings.* Washington, D.C.: Transportation Research Board.

(2)   AASHTO. (2010). *LRFD Bridge Design Specifications.* Washington, D.C.: American Association of State Highway and Transportation Officials.

(3)   ASCE. (1982). Fatigue Reliabilty: Variable Amplitude Loading. *Journal of the Structural Division, 108*(ST1), 47-69.

(4)   Li, Z., Chan, T., and Ko, J. (2001). Fatigue Analysis and Life Prediction of Bridges with Structural Health Monitoring Data - Part I: Methodology and Strategy. *International Journal of Fatigue, 23*, 45-53.

(5)   Fasl, J. (2013). *Estimating the Remaining Fatigue Life of Steel Bridges Using Field Measurements.* The University of Texas at Austin. Dissertation.

(6)   Fasl, J., Helwig, T., Wood, S. L., and Frank, F. (2012). Using Strain Data to Estimate the Remaining Fatigue Life of a Fracture-Critical Bridge. *Transportation Research Record, 2313*, 63-71.

(7)   AASHTO. (2011). *The Manual for Bridge Evaluation.* Washington, D.C.: American Association of State Highway and Transportation Officials.

(8)   Fasl, J. Helwig, T., and Wood, S. L. (2013). Probabilistic Method for Estimating Remaining Fatigue Life in Steel Bridges Using Measured Strain Data. *Journal of Civil Structural Health Monitoring, 3(4),* 317-324.